Stretchable Supercapacitors Based on Buckled Single-Walled Carbon Nanotube Macrofilms

By *Cunjiang Yu, Charan Masarapu, Jiepeng Rong, Bingqing Wei,** and *Hanqing Jiang**

Stretchable electronic devices, such as p–n diodes,[1] photovoltaic devices,[2,3] transistors,[4,5] and functional electronic eyes,[6] have been fabricated using buckled single-crystal (e.g., Si, GaAs) thin films supported by elastomeric substrates. Recently, carbon nanotube (CNT)-based highly conducting elastic composites[7,8] and stretchable graphene films[9] have been reported, which are suitable as interconnects in stretchable electronic devices. As an indispensable component of stretchable electronics, a stretchable power-source device should be able to accommodate large strains while retaining intact function. Of various power-source devices, supercapacitors have attracted great interest in recent years due to their high power and energy densities compared with lithium-ion batteries and conventional dielectric capacitors, respectively. The most active research in supercapacitors is the development of new electrode materials. Recently, CNTs have been studied as good candidates for electrode materials[10–16] because of several advantages, including a high surface area, nanoscale dimensions, and excellent electrical conductivity.

Here, we report stretchable supercapacitors based on periodically sinusoidal single-walled carbon nanotube (SWNT) macrofilms (a 2D network of randomly oriented SWNTs). The stretchable supercapacitors comprise two sinusoidal SWNT macrofilms as stretchable electrodes, an organic electrolyte, and a polymeric separator. Electrochemical tests were performed and the fabricated stretchable supercapacitors are found to possess energy and power densities comparable with those of supercapacitors using pristine SWNT macrofilms as electrodes. Remarkably, the electrochemical performance of the stretchable supercapacitors remains unchanged even under 30% applied tensile strain.

The preparation of the periodically sinusoidal SWNT macrofilms is of primary importance for stretchable supercapacitors. The synthesis of high-quality, purified, and functionalized SWNT macrofilms is, thus, an important preprocess, which has been presented elsewhere.[17] The purified SWNT macrofilm was then shaped to a sinusoidal form by following the steps shown in Figure 1a. The procedure introduced here (step i in Fig. 1a) involves the uniaxial prestretching (ε_{pre}) of an elastomeric substrate of a poly(dimethylsiloxane) (PDMS) slab ($\varepsilon_{pre} = \Delta L/L$ for length changed from L to $L + \Delta L$), followed by a chemical surface treatment to form a hydrophilic surface (see Experimental Section). The exposure of UV light introduces atomic oxygen, an activated species that reacts with PDMS and, thus, changes the

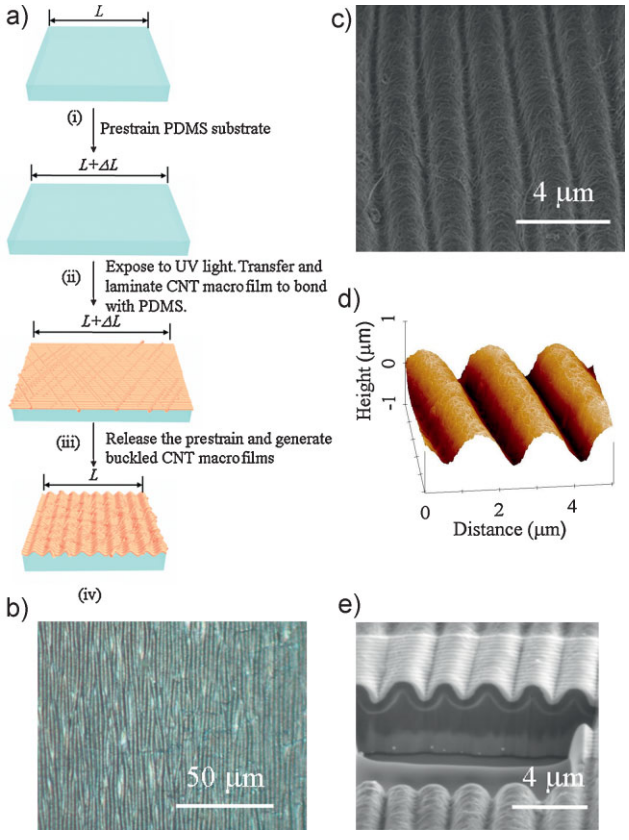

Figure 1. Fabrication steps of a buckled SWNT macrofilm on an elastomeric PDMS substrate. a) Illustration of the fabrication flow comprising surface treatment, transfer, and relaxation of the prestrained PDMS substrate. b) Optical microscopy image of a 50-nm-thick, buckled SWNT macrofilm on a PDMS substrate with 30% prestrain, where the well-defined periodic buckling structure is shown. c) SEM image of a buckled SWNT macrofilm. The buckling wavelength is 2 μm. d) AFM image of the buckling profile of the SWNT macrofilm. The buckling amplitude is 0.4 μm. e) SEM image of the buckled SWNT macrofilm/PDMS substrate interface, where the top white layer is a very thin layer of platinum that was sputtered onto the SWNT macrofilm in advance to prevent the SWNT macrofilm from damage during ion milling.

[*] Prof. H. Jiang, C. Yu
Department of Mechanical and Aerospace Engineering
Arizona State University
Tempe, AZ 85287 (USA)
E-mail: hanqing.jiang@asu.edu
Prof. B. Q. Wei, Dr. C. Masarapu, J. P. Rong
Department of Mechanical Engineering
University of Delaware
Newark, DE 19716 (USA)
E-mail: weib@udel.edu

DOI: 10.1002/adma.200901775

hydrophobic surface (dominated by $-OSi(CH_3)_2O-$ groups) to a hydrophilic surface (terminated with $-O_nSi(OH)_{4-n}$ functionalities).[18,19] The hydrophilic surface of PDMS is able to form strong chemical bonding through condensation reactions with various inorganic surfaces that have $-OH$ groups. The purified SWNT macrofilm with extensive $-OH$ groups was laminated and aligned against the prestrained, UV-treated PDMS substrate along the direction of the prestrain (step ii) to form covalent bonds ($-C-O-Si-$) through condensation reactions. Releasing the prestrain in the PDMS substrate leads to the spontaneous formation of periodically buckled patterns due to mechanical competition between the relatively stiff SWNT macrofilm and the compliant PDMS substrate (step iii). Figure 1b shows an optical microscopy image of a buckled SWNT film on a PDMS substrate, in which the prestrain is $\varepsilon_{pre} = 30\%$ and the thickness of the film is $h_{SWNT} = 50$ nm. Figure 1c and d shows tilted-view scanning electron microscopy (SEM) and atomic force microscopy (AFM) images of the buckled SWNT film on PDMS substrates. These images demonstrate uniform, periodic wavy patterns, with a wavelength of $\lambda = 2\,\mu m$ and an amplitude of $A = 0.4\,\mu m$.

The buckling wavelength and amplitude can be characterized by a nonlinear mechanics theory by modeling the SWNT macrofilm as linear elastic material laying on a semi-infinite compliant substrate, subject to large deformation (Eq. (1)).[20,21]

$$\lambda = \frac{\lambda_0}{(1+\varepsilon_{pre})(1+\xi)^{\frac{1}{3}}},\ A \approx \frac{A_0}{\sqrt{1+\varepsilon_{pre}}(1+\xi)^{\frac{1}{3}}} \quad (1)$$

$$A_0 = h\sqrt{\frac{\varepsilon_{pre}}{\varepsilon_c} - 1} \quad (2)$$

$$\lambda_0 = 2\pi h_{SWNT}\left[\frac{E_{SWNT}(1-\nu_{PDMS}^2)}{3E_{PDMS}(1-\nu_{SWNT}^2)}\right]^{\frac{1}{3}} \quad (3)$$

$$\varepsilon_c = \frac{1}{4}\left[\frac{3E_{PDMS}(1-\nu_{SWNT}^2)}{E_{SWNT}(1-\nu_{PDMS}^2)}\right]^{\frac{2}{3}} \quad (4)$$

$$\xi = \frac{5}{32}\varepsilon_{pre}(1+\varepsilon_{pre}) \quad (5)$$

λ_0 and A_0 are the wavelength and amplitude, respectively, based on small deformation theory.[22] ε_c is defined as the critical buckling strain, or the minimum strain needed to induce buckling; ξ represents the large deformation and geometrical nonlinearity in the substrate. E is the Young's modulus; ν is Poisson's ratio, and the subscripts refer to the SWNT macrofilm and PDMS substrate. When the following literature values[23,24] for the mechanical properties[25] ($E_{SWNT} = 4.5$ GPa, $\nu_{SWNT} = 0.3$, $E_{PDMS} = 2$ MPa, $\nu_{PDMS} = 0.49$) are used, the analytical solutions (Eq. 1) give $\lambda = 2.03\,\mu m$ and $A = 0.4\,\mu m$, which agrees very well with the experiments without any parameter fitting.

To verify a good interface between buckled SWNT films and PDMS substrates, which is important for the electrochemical performance, we examined the interface between buckled SWNT macrofilms and PDMS using an integrated focused ion beam (FIB) and an SEM system. Figure 1e shows an SEM image of the interface, where the top white layer is a very thin platinum layer that was sputtered onto the buckled SWNT macrofilm in advance to prevent damaging the films during ion milling. No apparent debonding between the buckled SWNT macrofilm and PDMS has been observed, indicating strong interfacial bonding even for a large prestrain (e.g., 30% in this image).

Since the maximum power of a supercapacitor is given by $P = V_i^2 / 4R$ (V_i is the initial voltage and R is the equivalent series resistance), the key factor to maintain a consistent power of

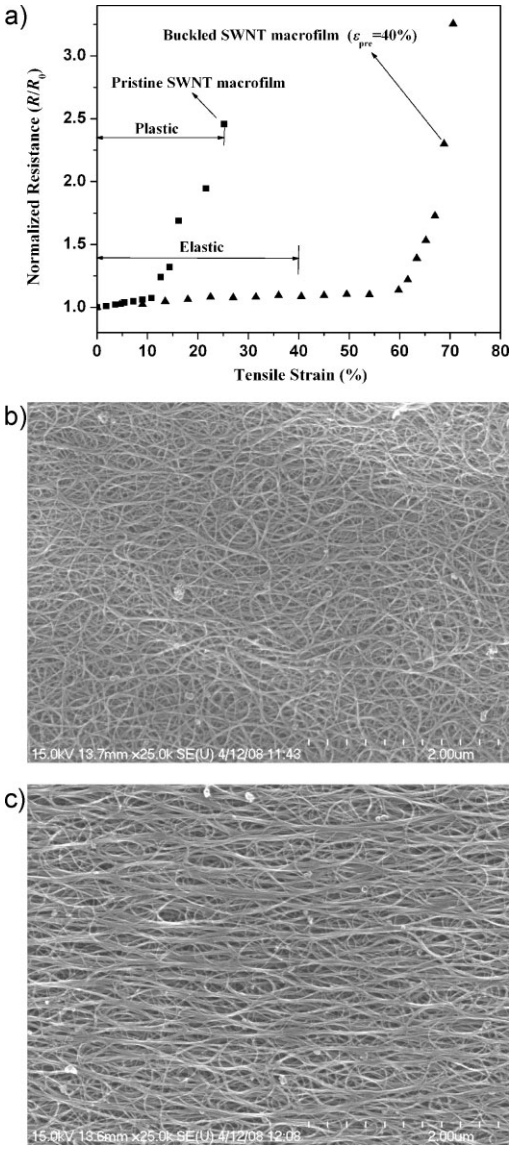

Figure 2. Normalized electrical resistances versus tensile strains of 50-nm-thick buckled and pristine SWNT macrofilms. a) The measurement of the buckled SWNT macrofilm is marked in triangle while that of the pristine SWNT macrofilm is marked in square. b) SEM image of a randomly aligned pristine SWNT macrofilm. c) SEM image of the film stretched by 10% tensile strain, which clearly shows the stretch-induced alignment.

stretchable supercapacitors is to keep the equivalent series resistance unvaried under mechanical stretch. It is expected that the buckled SWNT macrofilms have unchanged conductance under reversible stretch. To verify it, we measured the resistances of pristine and buckled SWNT macrofilms under stretch. In a SWNT film (either pristine or buckled), where the nanotubes are bundled together and these bundles, in turn, are highly entangled, the conduction of electrons in the film takes place through the bundles as well as by a hopping mechanism, where the electrons tunnel from one bundle to another. Figure 2a shows the normalized resistance at different strain levels, where R_0 is the resistance of the unstretched SWNT macrofilm. For the pristine SWNT macrofilm (thickness $h_{SWNT} = 50$ nm), the resistance (squares in Fig. 2a) first increases slowly when the tensile strain is less than about 10%. This can be explained by two mechanisms. On one hand, during stretch-induced alignment (Fig. 2c) of originally randomly distributed SWNTs (Fig. 2b), the overlap length (where the electrons tunnel from one bundle to another) increases and, therefore, the resistance decreases; on the other hand, the resistance increases due to the elongation of the SWNT macrofilms by the tensile strain. The competition of these two opposing mechanisms qualitatively leads to almost constant resistance up to 10%. Upon further stretch, however, the resistance increases significantly, which can be explained by a decrease of the overall overlap length and an increase of the film length due to tube sliding. It is also worth noting that this elongation is irreversible upon releasing the tensile strain because of the irreversible tube sliding.

Distinguished from the pristine SWNT macrofilms, buckled SWNT macrofilms exhibit excellent stretchability. As shown in Figure 2a (triangle), the resistance remains fairly unchanged for the buckled film (thickness = 50 nm) before the applied tensile strain reaches the prestrain (40%). Without changing the overall overlap length and the film length while stretched, the buckled SWNT macrofilms accommodate the applied tensile strains by simply increasing the buckling wavelength and decreasing the buckling amplitude, resulting in an unchanged resistance. More importantly, this stretchability is reversible within the prestrain range, similar to an accordion bellow. Once the applied strain reaches the prestrain of 40%, the buckled SWNT macrofilm resumes flat. Upon further stretching, the flattened SWNT macrofilm performs

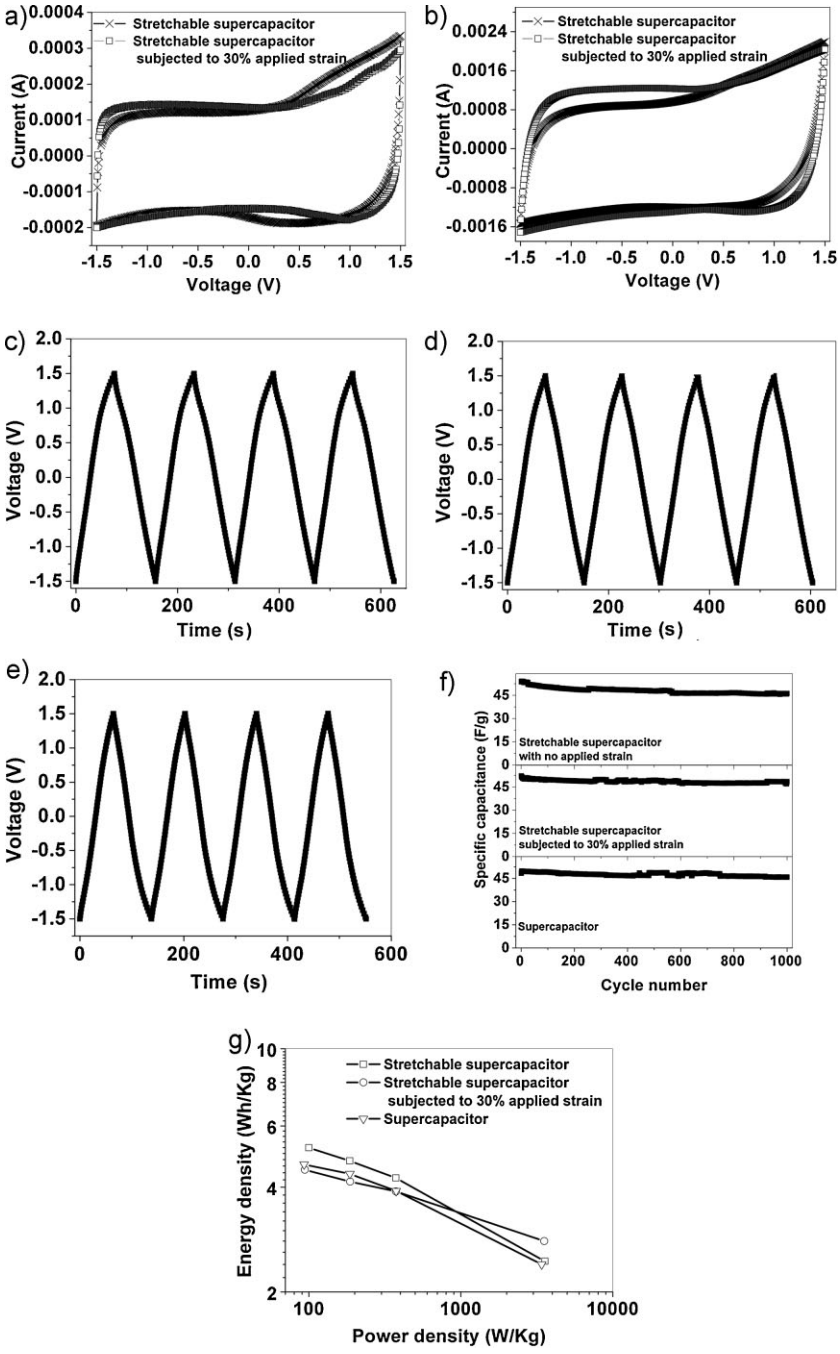

Figure 3. Measurements of stretchable supercapacitors subjected to 0 and 30% applied tensile strain, along with supercapacitors using the pristine SWNT film for comparison. a,b) Cyclic voltammograms of the stretchable supercapcitors measured at scan rates of 100 mV s^{-1} and 1000 mV s^{-1}, respectively. There is no significant deviation in the CVs of the stretchable supercapacitor with or without 30% applied strain. c–e) Charge–discharge cycles measured with a constant current density of 1 A g^{-1} for the stretchable supercapacitor subjected to 0 and 30% applied strain and for the supercapacitor with the pristine SWNT film, respectively. f) Long charge–discharge cycling at a constant current density of 1 A g^{-1} demonstrates the stability of the stretchable supercapacitor under 0 and 30% applied tensile strain. g) Energy and power densities of the supercapacitors calculated from the constant current density charge–discharge curves measured between 250 mA g^{-1} and 10 A g^{-1}. The values of the stretchable supercapacitor under 30% applied strain are very much comparable to the supercapacitor with the pristine SWNT films, indicating that the stretchable supercapacitor using the buckled SWNT films can be stretched up to 30% without any performance degradation.

in the same way as the pristine SWNT macrofilm. As indicated in Figure 2a, the electrical resistance experienced no remarkable change, even under 50% tensile strain, for the buckled SWNT macrofilm. Therefore, the buckled SWNT macrofilm is stretchable before flattening and its stretchability depends on the prestrains. Our studies have shown that the buckled SWNT macrofilm provides an excellent scenario to achieve stretchability and meanwhile retain electrical conductance, which is critical for stretchable supercapacitors.

To demonstrate the feasibility of the stretchable supercapacitors with almost invariant electrochemical performances (e.g., capacitance, power, and energy densities), supercapacitors with the buckled SWNT macrofilms as electrodes were assembled and their electrochemical behaviors were studied while strain ($\varepsilon_{applied}$) is applied. The buckled SWNT macrofilms in supercapacitors were formed by releasing the PDMS substrates with 30% prestrain. For comparison, the electrochemical performance of the supercapacitor assembled with pristine SWNT macrofilms as electrodes was also test. Figure 3a and b shows the cyclic voltammograms (CVs) of the stretchable supercapacitor measured at different scan rates. The CVs retained rectangular shape with ideal capacitive behavior even at a high scan rate of 1000 mV s^{-1} (Fig. 3b). No significant change was observed in the CVs of the stretchable supercapacitors with 0 and 30% applied strains. The cycling stability of the stretchable supercapacitors subjected to applied strains along with the supercapacitor assembled with the pristine SWNT macrofilms as electrodes is illustrated by galvanostatic charge–discharge with a constant current density of 1 A g^{-1} up to 1000 cycles (Fig. 3c–e). The initial specific capacitances calculated from the discharge slopes (Fig. 3c–e) were 54 F g^{-1} for the stretchable supercapacitor without applied strain (top frame in Fig. 3f) and 52 F g^{-1} for that subject to 30% applied strain (middle frame in Fig. 3f). These values are comparable to the specific capacitance (50 F g^{-1}) of the supercapacitor with the pristine SWNT macrofilms as electrodes (bottom frame in Fig. 3f). Remarkably, the specific capacitances of stretchable supercapacitors with or without applied strain do not alter even up to 1000 charge–discharge cycles, which concludes excellent electrochemical stability. In addition, the energy and power densities of the stretchable supercapacitors with or without applied strains do not have significant variation compared to those of the supercapacitor with the pristine SWNT macrofilms as shown in Figure 3g.

In summary, we have demonstrated supercapacitors of high stretchability, depending on the level of prestain applied to the PDMS substrate, whose electrochemical performances remain unchanged during mechanical stretch. We expect that stretchable supercapacitors will enlighten a broad area of stretchable energy-storage devices to be compatible with stretchable electronics.

Experimental

Preparation of PDMS Substrates: PDMS was prepared by mixing silicone-elastomer base and curing agent (Sylgard 184, Dow Corning) at the ratio of 10:1 by weight, pouring into a glass container, and baking at 100 °C for 45 min. Rectangular slabs of 1.5 × 6 cm were cut from the polymerized piece. The slab was rinsed with isopropyl alcohol (IPA) to remove contaminations and dried using a nitrogen gun. A custom-made stage was utilized to stretch the PDMS to specific strain levels. The prestrained PDMS substrate was subjected to a flood exposure by a UV light (low-pressure mercury lamp, BHK), which produces 185- and 254-nm radiation, for 150 s. The 185-nm radiation produces ozone, while the 254-nm radiation dissociates the ozone to O_2 and atomic oxygen to form a chemically activated surface.

Synthesis of SWNT Macrofilms: The growth of the SWNT films involved a simple floating chemical vapor deposition (CVD) method, in which a mixture of ferrocene and sulfur in the weight ratio 10:1 was controllably evaporated into the CVD tube reactor under argon/hydrogen atmosphere. Ferrocene acted as a carbon feedstock/catalyst and sulfur as an additive to promote SWNT growth to a high percentage. The CNT film possessed a hydrophobic surface as synthesized. A post purification, a combination of oxidation (heating in air at 450 °C for 1 h or immersion in 30% H_2O_2 solution for 72 h) and rinsing with diluted acid (37% HCl) [17,26], significantly reduced the amount of impurities and increased the functional groups (e.g., O=C−OH) within the film and, hence, altering the surface to become hydrophilic. The resulting hydrophilic surface highly benefited the strong interaction with the activated PDMS surface by providing sufficient −C−OH surface chemistry.

Supercapacitor Assembly and Electrochemical Measurements: The supercapacitor was assembled as a two-electrode system. A 1 M solution of tetraethylammonium tetrafluoroborate dissolved in propylene carbonate was used as the electrolyte. Two PDMS sheets with buckled SWNT films were pressed together with a filter paper in between that was soaked in the electrolyte. The SWNT films themselves acted as current collectors. Thin copper strips were placed at the edge of each SWNT-film electrode for electrical contact. The resistance measurements were done by placing two copper strips at the edges of the SWNT film that was attached to the PDMS substrate. The tensile strain was applied by holding the PDMS sheet on both sides at the location where the copper strips touch the SWNT film, so as to keep the electrical contact between the copper and SWNT intact during the application of the strain. The assembly was carried out in a glove box (Unilab, MBraun) filled with purified argon. The assembled supercapacitor was mounted on a custom-made stage. Cyclic voltammetry was carried out between the voltage window from −1.5 V to + 1.5 V using an Autolab Potentiostat/Galvanostat. Galvanostatic charge–discharge measurements were done using a four-channel Arbin system. First, all the electrochemical measurements on the supercapacitor with buckled SWNT film electrodes were carried out. Then, by using the custom-made stage, the stretchable supercapacitor was stretched by 30% tensile strain, where the SWNT macrofilms should become almost flattened and the measurements on the stretched supercapacitor were carried out. The specific capacitance (C) was calculated from the slope of the discharge capacitance (Eq. (6)), where I is the applied current and m is the average mass of the two SWNT film electrodes.

$$C = \frac{2I}{m(\frac{\Delta V}{\Delta t})} \tag{6}$$

The energy and power density were calculated by conducting galvanostatic charge–discharge cycling with constant current densities ranging from 250 mA g^{-1} to 10 A g^{-1}.

Acknowledgements

The authors thank Haifeng Zeng for assistance in preparing SWNT films. H.J. acknowledges the support from NSF CMMI-0824787 and 0844737. B.Q.W. is grateful for financial support from NSF CMMI-0824790.

Received: May 27, 2009
Published online: August 12, 2009

[1] D. Y. Khang, H. Q. Jiang, Y. Huang, J. A. Rogers, *Science* **2006**, *311*, 208.
[2] Y. G. Sun, W. M. Choi, H. Q. Jiang, Y. G. Y. Huang, J. A. Rogers, *Nat. Nanotechnol.* **2006**, *1*, 201.

[3] J. Yoon, A. J. Baca, S. I. Park, P. Elvikis, J. B. Geddes, L. F. Li, R. H. Kim, J. L. Xiao, S. D. Wang, T. H. Kim, M. J. Motala, B. Y. Ahn, E. B. Duoss, J. A. Lewis, R. G. Nuzzo, P. M. Ferreira, Y. G. Huang, A. Rockett, J. A. Rogers, *Nat. Mater.* **2008**, *7*, 907.

[4] D. H. Kim, J. H. Ahn, W. M. Choi, H. S. Kim, T. H. Kim, J. Z. Song, Y. G. Y. Huang, Z. J. Liu, C. Lu, J. A. Rogers, *Science* **2008**, *320*, 507.

[5] D. H. Kim, J. Z. Song, W. M. Choi, H. S. Kim, R. H. Kim, Z. J. Liu, Y. Huang, K. C. Hwang, Y. W. Zhang, J. A. Rogers, *Proc. Natl. Acad. Sci. USA* **2008**, *105*, 18675.

[6] H. C. Ko, M. P. Stoykovich, J. Z. Song, V. Malyarchuk, W. M. Choi, C. J. Yu, J. B. Geddes, J. L. Xiao, S. D. Wang, Y. G. Huang, J. A. Rogers, *Nature* **2008**, *454*, 748.

[7] T. Sekitani, H. Nakajima, H. Maeda, T. Fukushima, T. Aida, K. Hata, T. Someya, *Nat. Mater.* **2009**, *8*, 494.

[8] B. Y. Ahn, E. B. Duoss, M. J. Motala, X. Y. Guo, S. I. Park, Y. J. Xiong, J. Yoon, R. G. Nuzzo, J. A. Rogers, J. A. Lewis, *Science* **2008**, *323*, 1590.

[9] K. S. Kim, Y. Zhao, H. Jang, S. Y. Lee, J. M. Kim, K. S. Kim, J. H. Ahn, P. Kim, J. Y. Choi, B. H. Hong, *Nature* **2009**, *457*, 706.

[10] C. M. Niu, E. K. Sichel, R. Hoch, D. Moy, H. Tennent, *Appl. Phys. Lett.* **1997**, *70*, 1480.

[11] R. Z. Ma, J. Liang, B. Q. Wei, B. Zhang, C. L. Xu, D. H. Wu, *J. Power Sources* **1999**, *84*, 126.

[12] E. Frackowiak, S. Delpeux, K. Jurewicz, K. Szostak, D. Cazorla-Amoros, F. Beguin, *Chem. Phys. Lett.* **2002**, *361*, 35.

[13] A. B. Dalton, S. Collins, E. Munoz, J. M. Razal, V. H. Ebron, J. P. Ferraris, J. N. Coleman, B. G. Kim, R. H. Baughman, *Nature* **2003**, *423*, 703.

[14] F. Pico, J. M. Rojo, M. L. Sanjuan, A. Anson, A. M. Benito, M. A. Callejas, W. K. Maser, M. T. Martinez, *J. Electrochem. Soc.* **2004**, *151*, A831.

[15] Q. L. Chen, K. H. Xue, W. Shen, F. F. Tao, S. Y. Yin, W. Xu, *Electrochim. Acta* **2004**, *49*, 4157.

[16] V. L. Pushparaj, M. M. Shaijumon, A. Kumar, S. Murugesan, L. Ci, R. Vajtai, R. J. Linhardt, O. Nalamasu, P. M. Ajayan, *Proc. Natl. Acad. Sci. USA* **2007**, *104*, 13574.

[17] H. W. Zhu, B. Q. Wei, *Chem. Commun.* **2007**, 3042.

[18] M. Ouyang, C. Yuan, R. J. Muisener, A. Boulares, J. T. Koberstein, *Chem. Mater.* **2000**, *12*, 1591.

[19] D. C. Duffy, J. C. McDonald, O. J. A. Schueller, G. M. Whitesides, *Anal. Chem.* **1998**, *70*, 4974.

[20] H. Jiang, D.-Y. Khang, J. Song, Y. Sun, Y. Huang, J. A. Rogers, *Proc. Natl. Acad. Sci. USA* **2007**, *104*, 15607.

[21] J. Song, H. Jiang, Z. J. Liu, D. Y. Khang, Y. Huang, J. A. Rogers, C. Lu, C. G. Koh, *Int. J. Solids Struct.* **2008**, *45*, 3107.

[22] Z. Y. Huang, W. Hong, Z. Suo, *J. Mechan. Phys. Solids* **2005**, *53*, 2101.

[23] A. Bietsch, B. Michel, *J. Appl. Phys.* **2000**, *88*, 4310.

[24] Y. Hayamizu, T. Yamada, K. Mizuno, R. C. Davis, D. N. Futaba, M. Yumura, K. Hata, *Nat. Nanotechnol.* **2008**, *3*, 289.

[25] The Young's modulus of CNT macrofilms has large scattering depending on various synthesis methods. The estimated modulus ranges from 1 GPa to 8 GPa. Here the mean value of 4.5 GPa is used.

[26] J. Q. Wei, H. W. Zhu, Y. H. Li, B. Chen, Y. Jia, K. L. Wang, Z. C. Wang, W. J. Liu, J. B. Luo, M. X. Zheng, D. H. Wu, Y. Q. Zhu, B. Q. Wei, *Adv. Mater.* **2006**, *18*, 1695.